Neurospine 2024;21(1):330-341.
https://doi.org/10.14245/ns.2346994.497

Neurospine
pISSN 2586-6583 eISSN 2586-6591

Original Article

Exploring lncRNA Expression Patterns in Patients With Hypertrophied Ligamentum Flavum

Corresponding Author
Jianwei Chen
https://orcid.org/0000-0002-7750-9759

Department of Orthopedics, Baoshan Branch, Renji Hospital, School of Medicine, Shanghai Jiao Tong University, No. 1058, Huan Zhen Bei Rd., Shanghai 200444, China
Email: jwchenbone@126.com

Received: September 26, 2023
Revised: December 11, 2023
Accepted: December 13, 2023

Junling Chen[1,*], Guibin Zhong[2,*], Manle Qiu[2], Wei Ke[1], Jingsong Xue[1], Jianwei Chen[1,2]

[1]Department of Orthopedics, Baoshan Branch, Ren Ji Hospital, School of Medicine, Shanghai Jiao Tong University, Shanghai, China
[2]Department of Orthopedics, Ren Ji Hospital, School of Medicine Shanghai Jiao Tong University, Shanghai, China

*Junling Chen and Guibin Zhong contributed equally to this study as co-first authors.

Objective: Hypertrophy ligamentum flavum (LFH) is a common cause of lumbar spinal stenosis, resulting in significant disability and morbidity. Although long noncoding RNAs (lncRNAs) have been associated with various biological processes and disorders, their involvement in LFH remains not fully understood.
Methods: Human ligamentum flavum samples were analyzed using lncRNA sequencing followed by validation through quantitative real-time polymerase chain reaction. To explore the potential biological functions of differentially expressed lncRNA-associated genes, Gene Ontology (GO) and Kyoto Encyclopedia of Genes and Genomes (KEGG) pathway analyses were performed. We also studied the impact of lncRNA PARD3-AS1 on the progression of LFH *in vitro*.
Results: In the LFH tissues when compared to that in the nonhypertrophic ligamentum flavum (LFN) tissues, a total of 1,091 lncRNAs exhibited differential expression, with 645 upregulated and 446 downregulated. Based on GO analysis, the differentially expressed transcripts primarily participated in metabolic processes, organelles, nuclear lumen, cytoplasm, protein binding, nucleic acid binding, and transcription factor activity. Moreover, KEGG pathway analysis indicated that the differentially expressed lncRNAs were associated with the hippo signaling pathway, nucleotide excision repair, and nuclear factor-kappa B signaling pathway. The expression of PARD3-AS1, RP11-430G17.3, RP1-193H18.3, and H19 was confirmed to be consistent with the sequencing analysis. Inhibition of PARD3-AS1 resulted in the suppression of fibrosis in LFH cells, whereas the overexpression of PARD3-AS1 promoted fibrosis in LFH cells *in vitro*.
Conclusion: This study identified distinct expression patterns of lncRNAs that are linked to LFH, providing insights into its underlying mechanisms and potential prognostic and therapeutic interventions. Notably, PARD3-AS1 appears to play a significant role in the pathophysiology of LFH.

Keywords: Hypertrophied ligamentum flavum, Long noncoding RNAs, Lumbar spinal stenosis

INTRODUCTION

Lumbar spinal stenosis (LSS) is a prevalent condition, particularly among older adults, characterized by the constriction of the lumbar spinal canal. This constriction can lead to the compression of the spinal cord and/or nerve roots, resulting in pain, sensory changes, and limited mobility.[1] Hypertrophy ligamentum flavum (LFH) plays an important role in the occurrence and development of LSS.[2] LFH involves an increase in the thickness and stiffness of the LF, which is a yellow elastic connective tissue located between adjacent laminae. LFH is characterized by the loss of elastic fibers and the increase of collagen

fibers, leading to ligamentum flavum (LF) fibrosis, spinal canal stenosis, and compression of neural elements.[2-5] Actually, ligamentum flavum thickness is positively correlated with the degree of fibrosis, which is the main cause of LFH.[2,5-7] However, the exact mechanisms underlying LFH remain to be fully understood.

Long noncoding RNAs (lncRNAs) are noncoding RNA molecules longer than 200 nucleotides that influence gene expression at various levels, including transcription, post-transcriptional regulation, and epigenetic modulation.[8] The role of lncRNAs has been identified in diverse biological processes, including cell proliferation, apoptosis, and tumorigenesis.[9,10] LncRNAs have also been associated with musculoskeletal diseases, such as osteoarthritis,[11] intervertebral disc degeneration,[12] and Ossification of the ligamentum flavum.[13] lncRNAs are also involved in the pathological process of fibrosis of the lung,[14,15] liver,[16,17] kidney,[18,19] and heart.[20,21] Past studies in LFH have demonstrated that lncRNAs are significantly associated with LF thickness and fibrosis in LSS patients, such as lncXIST.[22] However, the understanding of lncRNAs in the context of LFH is still limited. The study of differentially expressed lncrnas in LF of LSS patients can facilitate further elucidation of the pathogenesis of LFH at the epigenetic level, which may provide new clues for the treatment of LFH. This study aimed to investigate the differential expression of lncRNAs in LF tissues obtained from individuals with LSS when compared to LFN samples. We employed lncRNA sequencing analysis to identify the altered lncRNAs and validated the findings using quantitative real-time polymerase chain reaction (qRT-PCR) in LF samples. Additionally, we conducted pathway analysis using Gene Ontology (GO) and Kyoto Encyclopedia of Genes and Genomes (KEGG) to determine the potential biological functions of the differentially expressed lncRNAs. Furthermore, we examined the impact of lncRNA PARD3-AS1 on the progression of LFH *in vitro*. Our findings may offer new insights into the mechanisms underlying LFH development and contribute to the development of novel diagnostic and therapeutic strategies for this disorder.

MATERIALS AND METHODS

1. Tissue Samples

We screened 30 patients with both LFH and lumbar disc herniation (LDH) from those with LSS symptoms. Clinical diagnosis indicates that both the affected areas of LFH and LDH in these patients require surgical treatment to remove LF. Informed consent was obtained from all patients. For the LFH samples, we determined the location of LFH disease through intraoperative inspection and biopsy and removed them. For the LFN samples, we used LF samples from LDH-affected areas with no evidence of LSS based on preoperative magnetic resonance imaging. The tissues were immediately frozen in liquid nitrogen upon collection and stored at -80°C until further analysis.

The ethics committee of Renji Hospital approved this study, which is consistent with the guidelines of the Declaration of Helsinki. All patients provided their written informed consent prior to study participation.

2. Histological Analyses

The ligamentum flavum tissues were fixed overnight in 4% paraformaldehyde (Beyotime, Shanghai, China), followed by embedding in paraffin using standard procedures. Serial sections with a thickness of 4 μm were prepared for staining with hematoxylin and eosin (HE) and Masson trichrome.

3. RNA Extraction and Sequencing

As previously described, lncRNA sequencing was performed on 3 LFH and LFN samples using TRIzol reagent (Invitrogen, Carlsbad, CA, USA).[23] The integrity of the RNA was assessed using NanoDrop ND-1000 (NanoDrop Thermo, Waltham, MA, USA). The Ribo-Zero ribosomal RNA removal kit (Illumina, San Diego, CA, USA) was used to remove ribosomal RNA, and strand-specific total RNA libraries were prepared using the TruSeq Stranded Total RNA Library Prep Kit (Illumina). Sequencing was performed by Cloud-Seq Biotech (Shanghai, China) on an Illumina HiSeq 2500 Sequencer (Illumina).

4. Bioinformatics Analysis

The high-quality reads were aligned to the human reference genome (UCSC hg19) using Hisat2 software (ver. 2.0.4). Fragments per kilobase of transcript per million mapped reads (FPKM) values for lncRNAs were obtained using the cuffdiff software (part of cufflinks). Fold change and p-values were calculated based on FPKM, and differentially expressed lncRNAs were identified using a volcano plot and fold-change filters. Hierarchical clustering was performed using the differentially expressed lncRNA data. GO enrichment and KEGG pathway analyses were conducted to explore the potential biological functions of the differentially expressed lncRNAs using GO and KOBAS software (the KEGG orthology-based annotation system).

5. Isolation of Primary LF Cells

LF cells were isolated following a previously described method. The LFH and LFN tissues were minced into small pieces measuring approximately 0.5–1 mm^3 and treated with 0.25% trypsin and 250 U/mL type I collagenase (Sigma-Aldrich, St. Louis, MO, USA) in T25 flasks. The resulting cells were cultured in Dulbecco's modified Eagle medium supplemented with 10% fetal bovine serum and 1% penicillin/streptomycin (Gibco, Waltham, MA, USA) at 37°C in a humidified incubator with 5% CO_2 until they attained confluency. The culture media was replenished every 3 days, and trypsin was used for cell detachment during passaging. LF cells obtained from the third passage were used for all experiments.

6. Plasmids and Transduction

To investigate the role of lncRNA PARD3-AS1 in LFH progression, *in vitro* experiments were conducted using human LFH cells obtained from the tissue samples. shRNAs targeting sequences shPARD3-AS1-1 (5′-CCTAACTCGGTCCACGTTCC-3′), shPARD3-AS1-2 (5′-GTTCCCTAACTCGGTCCACG-3′), shPARD3-AS1-3 (5′-CGTGGACCGAGTTAGGGAAC-3′), and PARD3-AS1 overexpressing plasmid (ex-PARD3-AS1) were purchased from Vigenebio (Shandong, China). LFH cells were transfected with shRNA sequences/negative control or overexpressing plasmid/empty vector (mock) using Lipofectamine 2000 (Invitrogen) according to the manufacturer's instructions. Transfection efficiency was assessed using qRT-PCR at 48-hour posttransfection.

7. Quantitative Reverse Transcription Polymerase Chain Reaction

Total RNA was extracted from LF tissues or cells using TRIzol reagents (Invitrogen), followed by reverse transcription. qPCR was performed on the Applied Biosystems 7300 Fast Real-Time PCR system (Applied Biosystems, Waltham, MA, USA) using the SYBR Green qPCR master mix (Qiagen, Shanghai, China). Glyceraldehyde 3-phosphate dehydrogenase (GAPDH) was used as an endogenous control. RNA expression was evaluated by the $2^{-\Delta\Delta CT}$ method.[24] Sequences of the primers used are listed in Table 1.

8. Western Blotting

Total cellular protein was extracted using the radioimmunoprecipitation lysis buffer with protease inhibitors (Beyotime). Protein levels in each sample were quantified using a bicinchoninic acid assay kit (Beyotime). These proteins were separated by 10% sodium dodecyl sulfate-polyacrylamide gel electrophoresis, and 40 μg of the proteins were subsequently transferred to polyvinylidene fluoride membranes.

The blots were blocked with 5% skim milk and incubated overnight at 4°C with primary antibodies. These antibodies (Abcam, Cambridge, UK) were prepared in 5% bovine serum albumin as follows: collagen I (1:1,500, ab279711); collagen III (1:1,500, ab6310); transforming growth factor (TGF)-β1 (1:1,500, ab215715), and GAPDH (1:5,000, ab8245).[25-28]

After incubation with suitable horseradish peroxidase-conjugated secondary antibodies for 1 hour, protein bands were visu-

Table 1. Primer sequences for quantitative real-time polymerase chain reaction analysis

Gene ID	Gene short name	Primer sequences	Length (bp)
ENSG00000226752	PSMD5-AS1	F: 5′-GACCCAAGATGGACTGCCTGTA-3′	157
		R: 5′-TAACATCACACAGTATAGTGCAGCC-3′	
ENSG00000257595	RP3-473L9.4	F: 5′-GGCTTTGCAGGGTACAGGCT-3′	175
		R: 5′-CAACAAATAACCTTCCCATCACC-3′	
ENSG00000130600	H19	F: 5′-CTCAGGAATCGGCTCTGGAAG-3′	73
		R: 5′-CCGATGGTGTCTTTGATGTTGG-3′	
ENSG00000226386	PARD3-AS1	F: 5′-CAGCATAAGGAATCCTAACGCG-3′	110
		R: 5′-GTTCGGGCGTCTGCGTTAA-3′	
ENSG00000271200	RP11-430G17.3	F: 5′-TGGGAAAAGTGGGCTGTGG-3′	142
		R: 5′-AATTTCCTTGATCTTGGGTCTCG-3′	
ENSG00000267653	RP1-193H18.3	F: 5′-CCCATCTCAAGAACTACCCACG-3′	184
		R: 5′-TGTCGGAGAAGTCTGAGGGCA-3′	
2597	GAPDH	F: 5′-GGAAGCTTGTCATCAATGGAAATC-3′	168
		R: 5′-TGATGACCCTTTTGGCTCCC-3′	

https://doi.org/10.14245/ns.2346994.497

alized using an enhanced chemiluminescence kit (Millipore, Darmstadt, Germany). Densitometric quantification was performed using ImageJ (National Institutes of Health, Bethesda, MD, USA), with GAPDH serving as a normalization control.

9. Statistical Analysis

The study data were analyzed using GraphPad Prism v8 (GraphPad Software, San Diego, CA, USA) and presented as the means ± standard deviation of 3 independent experiments. Differences in the groups were analyzed by Student t-tests or 1-way analysis of variance. A p-value of < 0.05 was considered statistically significant.

RESULTS

1. Differential Expression of lncRNAs in LFH and LFN Tissues

lncRNA expression patterns in patients with LFH were investigated by performing RNA sequencing (RNA-seq) on LFH tissue samples (n = 3) and compared with those of control LFN samples (n = 3). The histological examination of patient-derived LF specimens stained with HE showed disrupted fiber organization in the LFH tissues (Fig. 1A). Furthermore, Masson trichrome staining highlighted the increased abundance of collagen fibers in these LFH tissues (Fig. 1B). The RNA-seq analysis revealed that 1,091 lncRNAs exhibited differential expression between LFH and LFN tissues, and 645 upregulated and 446

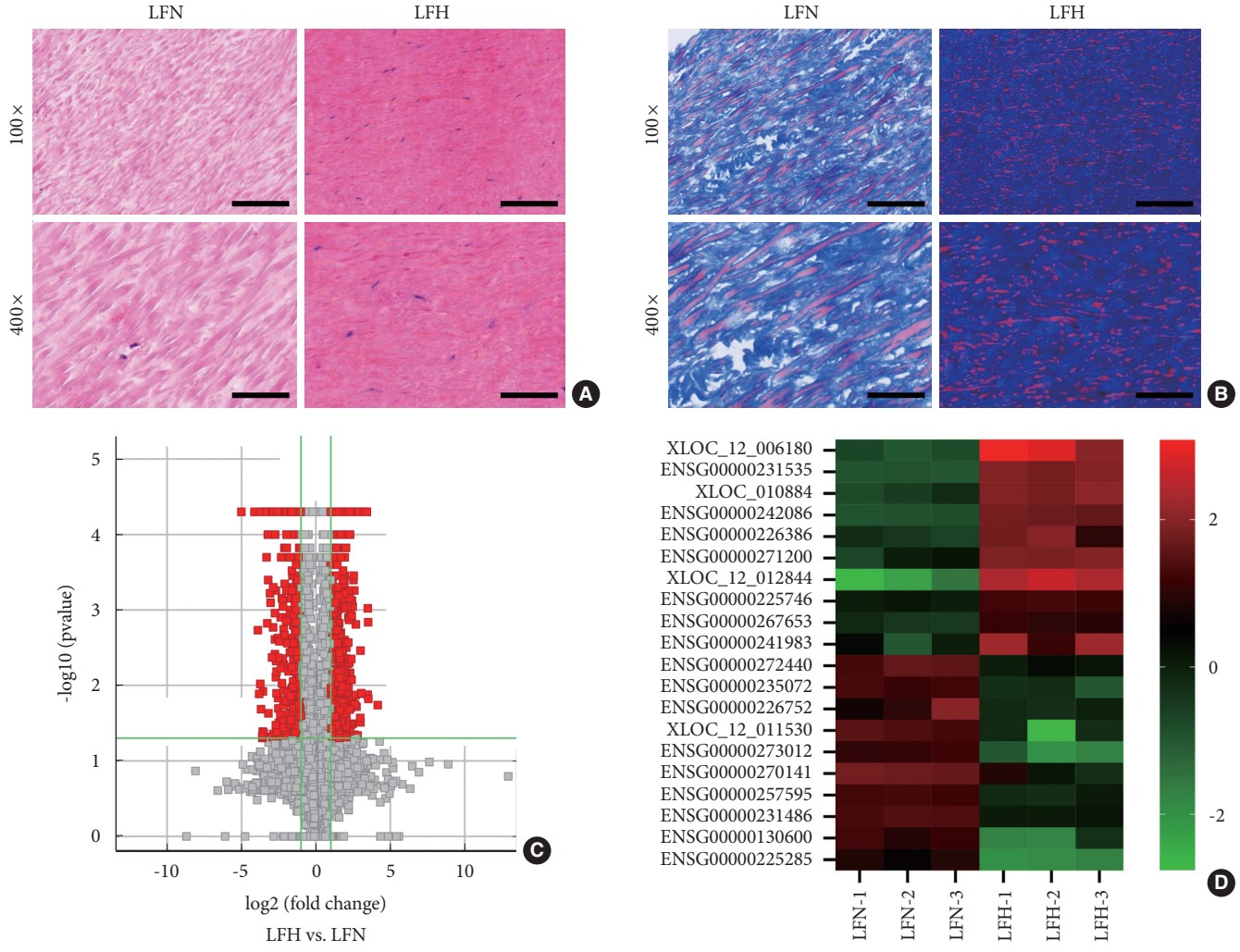

Fig. 1. Differences in the lncRNA expression profiles between LFH and LFN tissues. (A) Illustrative images depicting the results of hematoxylin and eosin staining. (B) Exemplary images of the results of Masson's trichrome staining. Scale bar = 100 μm or 20 μm. (C) Volcano plot displaying the RNA-seq data. (D) Heat maps depictng the varying expressions of distinct long noncoding RNAs in both LFN and LFH tissues. LFH, hypertrophy ligamentum flavum; LFN, nonhypertrophic ligamentum flavum.

Table 2. Differentially expressed long noncoding RNAs

Gene ID	Gene short name	Locus	Fold change	p-value	Differentially expressed
XLOC_l2_006180	XLOC_l2_006180	chr17:67573391-67899141	10.71	0.00005	Up
ENSG00000231535	LINC00278	chrY:2870952-2970313	9.91	0.00005	Up
XLOC_010884	XLOC_010884	chr14:80931125-80938379	9.53	0.00005	Up
ENSG00000242086	LINC00969	chr3:195384932-195467994	9.38	0.00005	Up
ENSG00000226386	PARD3-AS1	chr10:35104694-35105314	9.37	0.00005	Up
ENSG00000271200	RP11-430G17.3	chr1:62207669-62208096	8.55	0.00005	Up
XLOC_l2_012844	XLOC_l2_012844	chr6:1458801-1555481	8.16	0.01285	Up
ENSG00000225746	AL132709.5	chr14:101403737-101426536	8.13	0.00005	Up
ENSG00000267653	RP1-193H18.3	chr17:67410838-67539472	7.96	0.00345	Up
ENSG00000241983	RN7SL566P	chr19:39833035-39881835	7.93	0.03085	Up
ENSG00000272440	RP11-379F4.6	chr3:158413155-158413370	-32.28	0.00005	Down
ENSG00000235072	AC012074.2	chr2:25592041-25598714	-17.64	0.00005	Down
ENSG00000226752	PSMD5-AS1	chr9:123577773-123616651	-14.98	0.00185	Down
XLOC_l2_011530	XLOC_l2_011530	chr5:32925744-33298016	-14.10	0.01295	Down
ENSG00000273012	RP11-90B22.1	chr10:33630582-33630833	-13.55	0.00005	Down
ENSG00000270141	TERC	chr3:169482307-169482848	-13.38	0.00955	Down
ENSG00000257595	RP3-473L9.4	chr12:111807085-111841114	-12.13	0.04970	Down
ENSG00000231486	AC096579.7	chr2:89109983-89165653	-12.03	0.00005	Down
ENSG00000130600	H19	chr11:2016405-2022700	-11.97	0.04085	Down
ENSG00000225285	RP4-758J18.10	chr1:1365918-1369953	-11.90	0.00005	Down

downregulated lncRNAs were observed in LFH tissues (Fig. 1C; Supplementary Data 1). The top 10 upregulated and downregulated lncRNAs on the basis of fold change values are displayed in a heat map (Fig. 1D) and summarized in Table 2.

2. Functional Annotation of the Differentially Expressed Lncrnas

GO enrichment and KEGG pathway analyses were performed to identify the potential biological functions of the differentially expressed lncRNAs. The top 10 most-enriched GO terms were associated with biological processes, cellular components, and molecular functions (Fig. 2) as follows: The differentially expressed transcripts were mainly involved in metabolic processes of the biological process domain (Fig. 2A and D); the organelles, nuclear lumen, and cytoplasm of the cellular component domain (Fig. 2B and E); and protein binding, nucleic acid binding, and transcription factor activity of the molecular function domain (Fig. 2C and F).

The top 10 and 5 enriched KEGG pathways of upregulated and downregulated circular RNAs (circRNAs), respectively (Fig. 3), include the hippo signaling pathway and nucleotide excision repair for upregulated circRNAs (Fig. 3A) and SNARE interactions in vesicular transport and the nuclear factor (NF)-kappa B signaling pathway for downregulated circRNAs (Fig. 3B).

3. Validation of the Altered LncRNAs by qRT-PCR

To validate the differential expression of the altered lncRNAs identified by the sequencing analysis, we performed qRT-PCR on 30 paired tissue samples. The clinical and radiographic data are shown in Table 3. The upregulated and downregulated lncRNAs were arranged according to the fold change from high to low. Three randomly selected upregulated and downregulated lncRNAs from among the top 10 lncRNAs were arranged, namely PARD3-AS1 (Fig. 4A), RP11-430G17.3 (Fig. 4B), RP1-193H18.3 (Fig. 4C), PSMD5-AS1 (Fig. 4D), RP3-473L9.4 (Fig. 4E), and H19 (Fig. 4F), for validation. The qRT-PCR results showed that the expression patterns of PARD3-AS1, RP11-430G17.3, RP1-193H18.3, and H19 were consistent with the sequencing analysis results, which confirmed the differential expression of these lncRNAs. Among the 6 lncRNAs, PARD3-AS1 displayed the largest significant difference.

https://doi.org/10.14245/ns.2346994.497

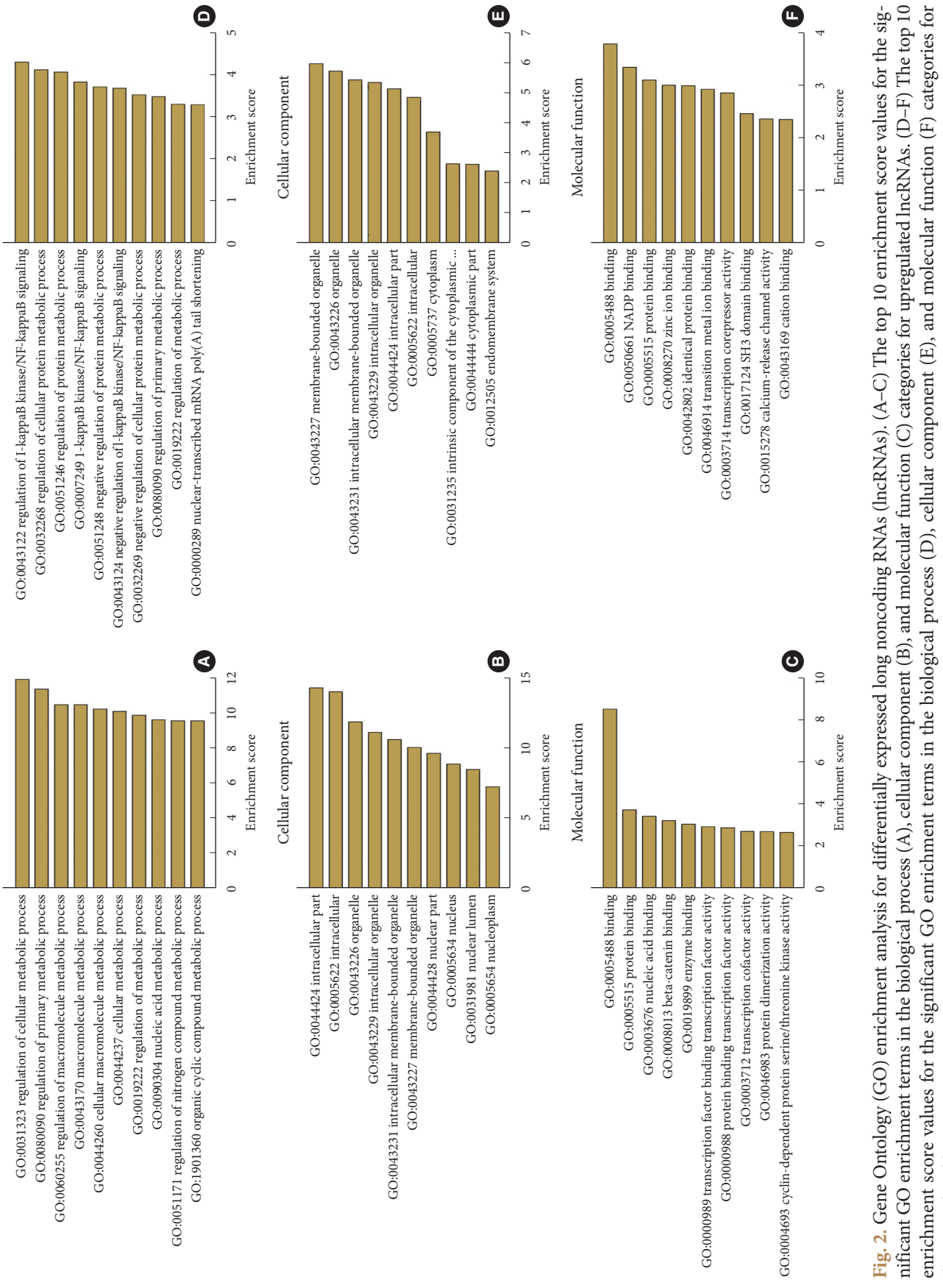

Fig. 2. Gene Ontology (GO) enrichment analysis for differentially expressed long noncoding RNAs (lncRNAs). (A–C) The top 10 enrichment score values for the significant GO enrichment terms in the biological process (A), cellular component (B), and molecular function (C) categories for upregulated lncRNAs. (D–F) The top 10 enrichment score values for the significant GO enrichment terms in the biological process (D), cellular component (E), and molecular function (F) categories for downregulated lncRNAs.

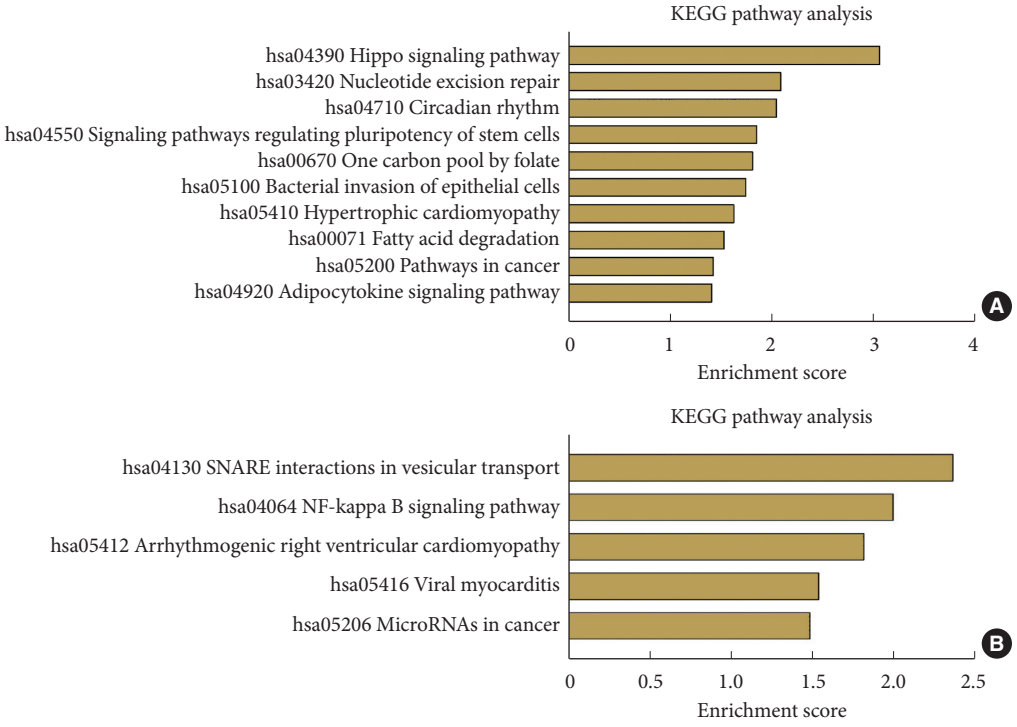

Fig. 3. The Kyoto Encyclopedia of Genes and Genomes (KEGG) pathway analysis for differentially expressed long noncoding RNAs (lncRNAs). (A) The top 10 enrichment score values for the significantly enriched pathways in upregulated lncRNAs. (B) The top 10 enrichment score values for the significantly enriched pathways in downregulated lncRNAs.

4. Effect of lncRNA PARD3-AS1 on LFH Progression *In Vitro*

To investigate the role of lncRNA PARD3-AS1 in LFH progression, we performed *in vitro* experiments using human LFH cells obtained from the tissue samples. First, we confirmed the transfection efficiency of the knockdown (Fig. 5A) and overexpression (Fig. 5B) of PARD3-AS1 by qRT-PCR. Among the tested shRNA constructs, shPARD3-AS1-3 produced the highest knockdown efficiency and was thus used in downstream experiments. The western blotting results showed that PARD3-AS1 knockdown decreased collagen I, collagen III, and TGF-β1 levels in the LFH cells compared with those in the control cells, while the levels were close to those in LFN cells. However, the PARD3-AS1 overexpression increased collagen I, collagen III, and TGF-β1 levels (Fig. 5C-F).

DISCUSSION

LFH is a major cause of LSS, leading to remarkable disability and morbidity.[2] Growing evidence shows that noncoding RNAs, including lncRNAs, play a role in the development and progression of various disorders, including spinal diseases.[9,29] Previous studies have investigated molecular mechanisms underlying LFH; however, the role of lncRNAs in LFH progression is only partially understood.[22,23,30,31] Here, we investigated the expression patterns of lncRNAs in LFH and LFN tissues by lncRNA sequencing. A total of 1,091 differentially expressed lncRNAs were identified in the LFH and LFN tissues, of which 645 were upregulated and 446 were downregulated.

The differentially expressed lncRNAs were analyzed for their biological functions by performing GO enrichment and KEGG pathway analyses. The GO analysis revealed that these lncRNAs were mainly associated with metabolic processes, organelles, nuclear lumen, cytoplasm, protein binding, nucleic acid binding, and transcription factor activity. These results are consistent with those of previous studies that have implicated alterations in cellular metabolism,[32] organelle function,[33] and transcriptional regulation[34,35] in LFH pathogenesis. Furthermore, the KEGG pathway analysis showed several signaling pathways that might be associated with the differentially expressed lncRNAs, including the hippo signaling pathway, nucleotide excision repair, SNARE interactions in vesicular transport, and the NF-kappa B signaling pathway. The hippo signaling pathway plays a critical role in tissue growth and regeneration,[36-38] whereas nucleotide excision repair is involved in DNA damage repair.[39,40] SNARE interactions in vesicular transport are related to synaptic transmission and neurodegenerative diseases,[41-43]

 https://doi.org/10.14245/ns.2346994.497

Table 3. Clinical and radiographic data

No.	Age (yr)	Sex	Diagnosis	Level		LF thickness (mm)	
				LFH	LDH	LFH	LDH
1	71	Male	LFH+LDH	L4–5	L5–S1	6.13	2.05
2	78	Female	LFH+LDH	L5–S1	L4–5	5.75	1.96
3	68	Female	LFH+LDH	L4–5	L5–S1	5.52	1.92
4	56	Male	LFH+LDH	L4–5	L5–S1	5.26	1.75
5	80	Female	LFH+LDH	L5–S1	L4–5	6.74	2.36
6	69	Male	LFH+LDH	L5–S1	L4–5	6.33	2.34
7	76	Male	LFH+LDH	L5–S1	L4–5	7.18	2.43
8	70	Female	LFH+LDH	L4–5	L3–4	5.07	1.65
9	76	Female	LFH+LDH	L5–S1	L4–5	6.38	2.14
10	72	Female	LFH+LDH	L5–S1	L4–5	6.50	2.25
11	74	Female	LFH+LDH	L4–5	L5–S1	6.58	2.36
12	59	Male	LFH+LDH	L4–5	L3–4	5.88	2.03
13	74	Male	LFH+LDH	L5–S1	L4–5	4.78	1.58
14	73	Female	LFH+LDH	L4–5	L5–S1	7.05	2.43
15	76	Female	LFH+LDH	L5–S1	L4–5	5.25	1.73
16	65	Male	LFH+LDH	L4–5	L5–S1	5.08	1.70
17	63	Male	LFH+LDH	L4–5	L5–S1	5.54	1.89
18	75	Female	LFH+LDH	L5–S1	L4–5	5.65	1.86
19	70	Male	LFH+LDH	L4–5	L3–4	5.28	1.85
20	59	Female	LFH+LDH	L5–S1	L4–5	5.23	1.78
21	71	Male	LFH+LDH	L5–S1	L4–5	5.52	1.85
22	73	Female	LFH+LDH	L5–S1	L4–5	6.21	2.14
23	74	Male	LFH+LDH	L4–5	L5–S1	6.56	2.33
24	81	Female	LFH+LDH	L5–S1	L4–5	5.05	1.68
25	72	Female	LFH+LDH	L5–S1	L4–5	4.76	1.53
26	75	Male	LFH+LDH	L4–5	L5–S1	4.96	1.62
27	65	Female	LFH+LDH	L4–5	L5–S1	5.39	1.74
28	75	Male	LFH+LDH	L4–5	L5–S1	5.15	1.66
29	77	Female	LFH+LDH	L5–S1	L4–5	5.73	1.87
30	74	Female	LFH+LDH	L5–S1	L4–5	5.45	1.82

LFH, hypertrophy ligamentum flavum; LFN, nonhypertrophic ligamentum flavum.

whereas the NF-kappa B signaling pathway is associated with inflammation and immune responses.[44,45] However, the specific roles of these pathways in LFH warrant further investigation.

The qRT-PCR results confirmed the expression patterns of PARD3-AS1, RP11-430G17.3, RP1-193H18.3, and H19, which were consistent with the sequencing analysis results. The investigation of the effect of lncRNA PARD3-AS1 knockdown/overexpression on the progression of LFH *in vitro* showed that PARD3-AS1 knockdown decreased the levels of fibrosis-related proteins (collagen I, collagen III, and TGF-β1) in the LFH cells, whereas PARD3-AS1 overexpression increased the levels these proteins. Past studies have demonstrated that collagen I and collagen III are representative fibrotic products.[25] TGF-β promotes collagen production and induces fibrosis in LF cells.[26-28] These results suggest that PARD3-AS1 may significantly affect the underlying processes and pathophysiology of LFH.

Past data has demonstrated that PARD3-AS1 is highly upregulated in the blood vessels of patients with atherosclerotic plaque formation (APF).[46] PARD3-AS1 is one of the unique genes associated with arterial spasm due to reduced blood flow.[47] Past

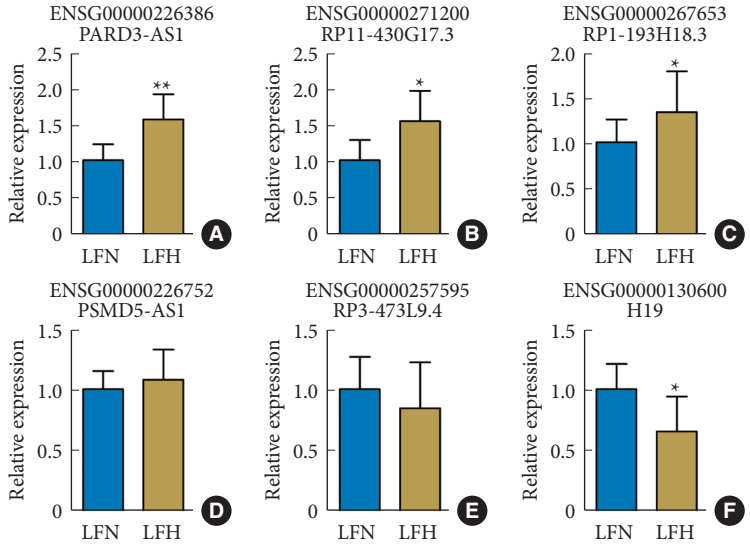

Fig. 4. Six chosen long noncoding RNAs were verified through qRT-PCR. (A) PARD3-AS1. (B) RP11-430G17.3. (C) RP1-193H18.3. (D) PSMD5-AS1. (E) RP3-473L9.4. (F) H19. LFH, hypertrophy ligamentum flavum; LFN, nonhypertrophic ligamentum flavum. $^{**}p < 0.05$, $^{*}p < 0.01$ when compared to the LFN group.

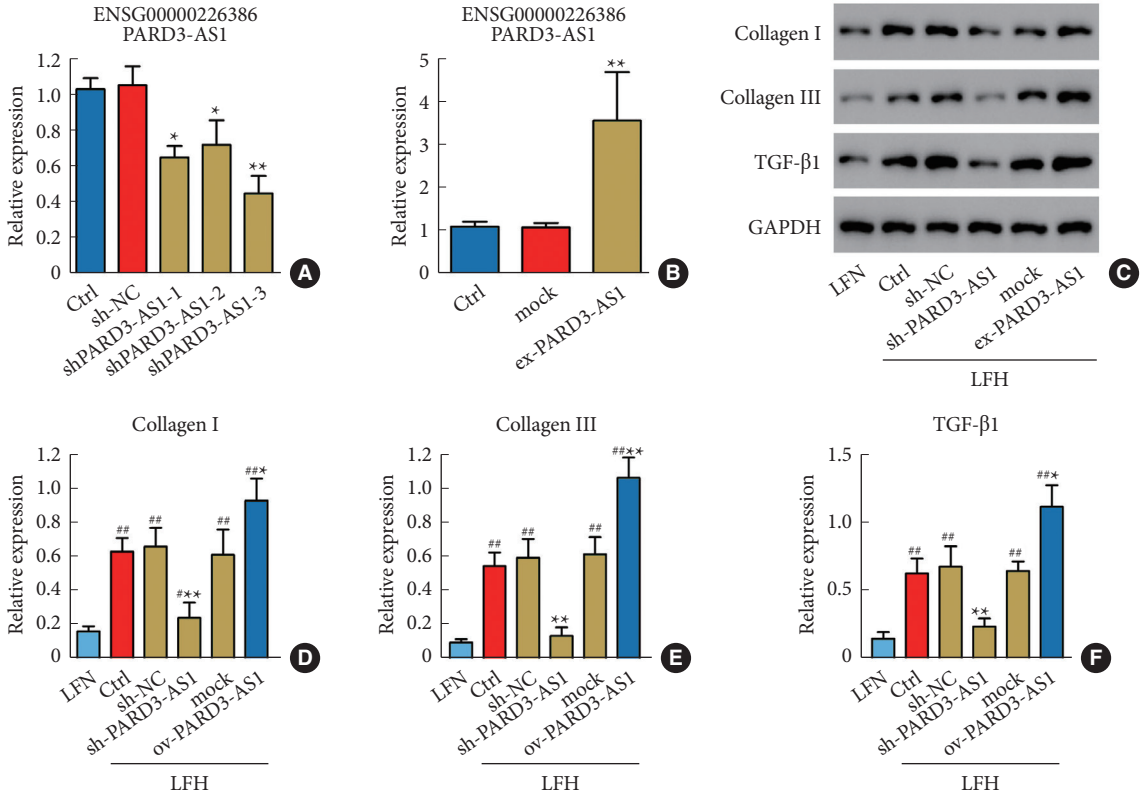

Fig. 5. Inhibition of PARD3-AS1 reduces fibrosis in ligamentum flavum cells derived from the LFH tissues. Quantitative real-time polymerase chain reaction was performed to analyze the PARD3-AS1 knockdown (A) and overexpression (B). (C–F) The expression of collagen I, collagen III, and TGF-β1 was evaluated through Western blotting. A significant difference was observed in comparison to control cells (Ctrl), with $^{*}p < 0.05$ and $^{**}p < 0.01$. A significant difference was observed in comparison to LFN cells, with $^{\#}p < 0.05$ and $^{\#\#}p < 0.01$. LFH, hypertrophy ligamentum flavum; LFN, nonhypertrophic ligamentum flavum; TGF, transforming growth factor; sh-NC, shRNA sequences/negative control.

https://doi.org/10.14245/ns.2346994.497

studies have indicated that vascular disease is one of the contributing factors to spinal degenerative diseases.[48] Patients with LSS are often complicated by peripheral artery diseases (PADs) and aortic diseases based on atherosclerosis (AS).[49] APF can reduce the blood supply to the lumbar spine and its surrounding structures, hinder the nutrition acquisition of the intervertebral disc, and induce disc degeneration and pain.[50] It is thus speculated that PARD3-AS1 may have a regulatory role between APF and LSS, and PARD3-AS1 is expected to provide a therapeutic target for spinal degenerative diseases induced by vascular diseases. Exploring the mechanism of PARD3-AS1 involvement in LSS can facilitate the elucidation of the pathogenesis of angiomatoid fibrous histiocytoma from the perspective of vascular diseases. The present findings suggest that PARD3-AS1 can promote the synthesis of fibrosis-related proteins in LF and thereby provide a therapeutic clue for LSS patients complicated with vascular diseases, such as APF and PAD. In the future, exploring the mechanism of PARD3-AS1 regulating LFH and its relationship with blood diseases can be used as a new research direction.

CONCLUSION

In this study, we identified specific lncRNA expression patterns associated with enlarged LF in patients with LSS. The differentially expressed lncRNAs might be associated with LFH development via diverse biological processes and pathways, offering a basis for potential prognostic and treatment options for the patients. PARD3-AS1 might have a significant effect on the underlying processes and pathophysiology of LFH and needs further investigation. However, the present study has some limitations, such as a small sample size and the lack of functional experiments *in vivo*. Thus, studies with larger sample sizes and animal models are warranted to verify our findings and explore the specific roles of altered lncRNAs and genes in LFH pathogenesis.

NOTES

Supplementary Material: Supplementary Data 1 can be found via https://doi.org/10.14245/ns.2346994.497.

Conflict of Interest: The authors have nothing to disclose.

Funding/Support: The study was supported by the Shanghai Baoshan District Science and Technology Innovation Special Fund Project (No: 20-E-33), Scientific Research Project of Shanghai Municipal Health Commission (No. 202040370) and Clinical Research Innovation Cultivation Fund of Baoshan Branch of Renji Hospital Affiliated to Shanghai Jiao Tong University School of Medicine (2023-rbcxjj-004).

Author Contribution: Conceptualization: Junling C, GZ, Jianwei C; Data curation: Junling C, MQ, WK, JX; Formal analysis: MQ, WK, JX; Funding acquisition: GZ; Methodology: Junling C, WK, JX, Jianwei C; Project administration: Junling C, GZ, Jianwei C; Writing - original draft: Junling C, MQ, JX; Writing - review & editing: Jianwei C.

ORCID

Jianwei Chen: 0000-0002-7750-9759

REFERENCES

1. Ma XL, Zhao XW, Ma JX, et al. Effectiveness of surgery versus conservative treatment for lumbar spinal stenosis: a system review and meta-analysis of randomized controlled trials. Int J Surg 2017;44:329-38.
2. Sun C, Zhang H, Wang X, et al. Ligamentum flavum fibrosis and hypertrophy: molecular pathways, cellular mechanisms, and future directions. FASEB J 2020;34:9854-68.
3. Kaye AD, Edinoff AN, Temple SN, et al. A comprehensive review of novel interventional techniques for chronic pain: spinal stenosis and degenerative disc disease-MILD percutaneous image guided lumbar decompression, vertiflex interspinous spacer, MinuteMan G3 interspinous-interlaminar fusion. Adv Ther 2021;38:4628-45.
4. Wettasinghe MC, Gamage L, Wickramasinghe ND. Hypertrophied posterior longitudinal ligament and ligamentum flavum causing myelopathy: a case report and literature review. Spinal Cord Ser Cases 2023;9:7.
5. Zhong ZM, Zha DS, Xiao WD, et al. Hypertrophy of ligamentum flavum in lumbar spine stenosis associated with the increased expression of connective tissue growth factor. J Orthop Res 2011;29:1592-7.
6. Sairyo K, Biyani A, Goel VK, et al. Lumbar ligamentum flavum hypertrophy is due to accumulation of inflammation-related scar tissue. Spine (Phila Pa 1976) 2007;32:E340-7.
7. Sairyo K, Biyani A, Goel V, et al. Pathomechanism of ligamentum flavum hypertrophy: a multidisciplinary investigation based on clinical, biomechanical, histologic, and biologic assessments. Spine (Phila Pa 1976) 2005;30:2649-56.
8. Mattick JS, Amaral PP, Carninci P, et al. Long non-coding RNAs: definitions, functions, challenges and recommendations. Nat Rev Mol Cell Biol 2023;24:430-47.

9. Fang Y, Liu J. Novel regulatory role of non-coding RNAs in ankylosing spondylitis. Front Immunol 2023;14:1131355.
10. Ahangar Davoodi N, Najafi S, Naderi Ghale-Noie Z, et al. Role of non-coding RNAs and exosomal non-coding RNAs in retinoblastoma progression. Front Cell Dev Biol 2022;10:1065837.
11. Ji ML, Li Z, Hu XY, et al. Dynamic chromatin accessibility tuning by the long noncoding RNA ELDR accelerates chondrocyte senescence and osteoarthritis. Am J Hum Genet 2023;110:606-24.
12. Li G, Ma L, He S, et al. WTAP-mediated m^6A modification of lncRNA NORAD promotes intervertebral disc degeneration. Nat Commun 2022;13:1469.
13. Zhang B, Chen G, Chen X, et al. Integrating bioinformatic strategies with real-world data to infer distinctive immunocyte infiltration landscape and immunologically relevant transcriptome fingerprints in ossification of ligamentum flavum. J Inflamm Res 2021;14:3665-85.
14. Huang C, Yang Y, Liu L. Interaction of long noncoding RNAs and microRNAs in the pathogenesis of idiopathic pulmonary fibrosis. Physiol Genomics 2015;47:463-9.
15. Zhou WQ, Wang P, Shao QP, et al. Lipopolysaccharide promotes pulmonary fibrosis in acute respiratory distress syndrome (ARDS) via lincRNA-p21 induced inhibition of Thy-1 expression. Mol Cell Biochem 2016;419:19-28.
16. Yu F, Guo Y, Chen B, et al. LincRNA-p21 Inhibits the Wnt/β-catenin pathway in activated hepatic stellate cells via sponging microRNA-17-5p. Cell Physiol Biochem 2017;41:1970-80.
17. Fu N, Zhao SX, Kong LB, et al. LncRNA-ATB/microRNA-200a/β-catenin regulatory axis involved in the progression of HCV-related hepatic fibrosis. Gene 2017;618:1-7.
18. Wang M, Wang S, Yao D, et al. A novel long non-coding RNA CYP4B1-PS1-001 regulates proliferation and fibrosis in diabetic nephropathy. Mol Cell Endocrinol 2016;426:136-45.
19. Wang M, Yao D, Wang S, et al. Long non-coding RNA ENSMUST00000147869 protects mesangial cells from proliferation and fibrosis induced by diabetic nephropathy. Endocrine 2016;54:81-92.
20. Wang K, Liu F, Zhou LY, et al. The long noncoding RNA CHRF regulates cardiac hypertrophy by targeting miR-489. Circ Res 2014;114:1377-88.
21. Han P, Li W, Lin CH, et al. A long noncoding RNA protects the heart from pathological hypertrophy. Nature 2014;514:102-6.
22. Cao Y, Li J, Qiu S, et al. LncRNA XIST facilitates hypertrophy of ligamentum flavum by activating VEGFA-mediated autophagy through sponging miR-302b-3p. Biol Direct 2023;18:25.
23. Chen J, Yu X, Qiu M, et al. Circular RNA expression profile in patients with lumbar spinal stenosis associated with hypertrophied ligamentum flavum. Spine (Phila Pa 1976) 2021;46:E916-25.
24. Larionov A, Krause A, Miller W. A standard curve based method for relative real time PCR data processing. BMC Bioinformatics 2005;6:62.
25. Jeong D, Lee MA, Li Y, et al. Matricellular protein CCN5 reverses established cardiac fibrosis. J Am Coll Cardiol 2016;67:1556-68.
26. Park JB, Lee JK, Park SJ, et al. Hypertrophy of ligamentum flavum in lumbar spinal stenosis associated with increased proteinase inhibitor concentration. J Bone Joint Surg Am 2005;87:2750-7.
27. Löhr M, Hampl JA, Lee JY, et al. Hypertrophy of the lumbar ligamentum flavum is associated with inflammation-related TGF-β expression. Acta Neurochirurgica 2011;153:134-41.
28. Wang S, Qu Y, Fang X, et al. Decorin: a potential therapeutic candidate for ligamentum flavum hypertrophy by antagonizing TGF-β1. Exp Mol Med 2023;55:1413-23.
29. Jiang C, Chen Z, Wang X, et al. The potential mechanisms and application prospects of non-coding RNAs in intervertebral disc degeneration. Front Endocrinol (Lausanne) 2022;13:1081185.
30. Zhang K, Wang X, Zeng LT, et al. Circular RNA PDK1 targets miR-4731-5p to enhance TNXB expression in ligamentum flavum hypertrophy. FASEB J 2023;37:e22877.
31. Chen J, Liu Z, Wang H, et al. SIRT6 enhances telomerase activity to protect against DNA damage and senescence in hypertrophic ligamentum flavum cells from lumbar spinal stenosis patients. Aging (Albany NY) 2021;13:6025-40.
32. Hsu YC, Chuang HC, Tsai KL, et al. Administration of N-acetylcysteine to regress the fibrogenic and proinflammatory effects of oxidative stress in hypertrophic ligamentum flavum cells. Oxid Med Cell Longev 2022;2022:1380353.
33. Gu Y, Yu W, Qi M, et al. Identification and validation of hub genes and pathways associated with mitochondrial dysfunction in hypertrophy of ligamentum flavum. Front Genet 2023;14:1117416.
34. Duan Y, Li J, Qiu S, et al. TCF7/SNAI2/miR-4306 feedback loop promotes hypertrophy of ligamentum flavum. J Transl Med 2022;20:468.
35. Zheng Z, Ao X, Li P, et al. CRLF1 Is a key regulator in the ligamentum flavum hypertrophy. Front Cell Dev Biol 2020;

 https://doi.org/10.14245/ns.2346994.497

8:858.
36. Ma S, Meng Z, Chen R, et al. The Hippo pathway: biology and pathophysiology. Annu Rev Biochem 2019;88:577-604.
37. Meng Z, Li FL, Fang C, et al. The Hippo pathway mediates Semaphorin signaling. Sci Adv 2022;8:eabl9806.
38. Kim CW, Yoon Y, Kim MY, et al. 12-O-tetradecanoylphorbol-13-acetate reduces activation of hepatic stellate cells by inhibiting the Hippo pathway transcriptional coactivator YAP. Cells 2022;12:91.
39. Wang S, Wang X, Sun J, et al. Down-regulation of DNA key protein-FEN1 inhibits OSCC growth by affecting immunosuppressive phenotypes via IFN-γ/JAK/STAT-1. Int J Oral Sci 2023;15:17.
40. Moretton A, Kourtis S, Gañez Zapater A, et al. A metabolic map of the DNA damage response identifies PRDX1 in the control of nuclear ROS scavenging and aspartate availability. Mol Syst Biol 2023;19:e11267.
41. Nenov MN, Laezza F, Haidacher SJ, et al. Cognitive enhancing treatment with a PPARγ agonist normalizes dentate granule cell presynaptic function in Tg2576 APP mice. J Neurosci 2014;34:1028-36.
42. Lévêque C, Maulet Y, Wang Q, et al. A role for the V0 sector of the V-ATPase in neuroexocytosis: exogenous V0d blocks complexin and SNARE interactions with V0c. Cells 2023;12:750.
43. Kim JK, Jha NN, Awano T, et al. A spinal muscular atrophy modifier implicates the SMN protein in SNARE complex assembly at neuromuscular synapses. Neuron 2023;111:1423-39.e4.
44. Chen S, Kong J, Wu S, et al. Targeting TBK1 attenuates ocular inflammation in uveitis by antagonizing NF-κB signaling. Clin Immunol 2023;246:109210.
45. Aqdas M, Sung MH. NF-κB dynamics in the language of immune cells. Trends Immunol 2023;44:32-43.
46. Li D, Ma Y, Deng W, et al. Construction and analysis of lncRNA-associated ceRNA network in atherosclerotic plaque formation. Biomed Res Int 2022;2022:4895611.
47. Rudy R. Genetic and epigenetic signatures in cerebrovascular disease [dissertation]. Boston (MA_: Harvard Medical School; 2019.
48. Beckworth WJ, Holbrook JF, Foster LG, et al. Atherosclerotic disease and its relationship to lumbar degenerative disk disease, facet arthritis, and stenosis with computed tomography angiography. PM R 2018;10:331-7.
49. Uesugi K, Sekiguchi M, Kikuchi S, et al. Lumbar spinal stenosis associated with peripheral arterial disease: a prospective multicenter observational study. J Orthop Sci 2012;17:673-81.
50. Rajasekaran S, Naresh-Babu J, Murugan S. Review of postcontrast MRI studies on diffusion of human lumbar discs. J Magn Reson Imaging 2007;25:410-8.